Core-level lineshapes in photoemission from transition-metal intercalates of TaS_2

1989 J. Phys.: Condens. Matter 1 6865

(http://iopscience.iop.org/0953-8984/1/38/011)

J. Phys.: Condens. Matter 1 (1989) 6865–6875. Printed in the UK

Core-level lineshapes in photoemission from transition-metal intercalates of TaS_2

J A Scarfe and H P Hughes
Physics and Chemistry of Solids, Cavendish Laboratory, University of Cambridge, Cambridge CB3 0HE, UK

Received 21 February 1989

Abstract. The photoemission lineshapes of the Ta 4f levels in 2H-TaS_2 and its intercalates $Mn_{1/4}TaS_2$ and $Co_{1/3}TaS_2$ have been studied using synchrotron radiation. The peaks show marked asymmetries because of the many-electron screening response to the core-hole potential. The different lineshapes are discussed in terms of the rigid band model of the electronic structure of the intercalates, and of the effects of charge transfer into the narrow conduction band on the many-electron response. Calculations of the lineshapes using a simple model for the conduction band density of states allow the experimental lineshapes to be understood in terms of intrinsic losses through multiple excitations within the narrow conduction band, together with some extrinsic plasma losses.

1. Introduction

The group-V transition-metal dichalcogenides are materials that crystallise in a layered structure; for TaS_2, each layer consists of a sheet of Ta atoms arranged in a hexagonal array, sandwiched between two similar hexagonal sheets of S atoms such that each Ta atom is surrounded by a trigonal prism of S atoms [1, 2]. The layers are then stacked in sequences that can produce a number of different polytypes. The principal electronic bonding is within the layer, while inter-layer bonding is weak and generally described as van der Waals bonding. Because of their layered structure, these materials exhibit a quasi-two-dimensional character in many of their properties, and this two-dimensionality is also reflected in their electronic structure. The weak interlayer bonding means that other species of atoms or molecules can be intercalated between the layers, and substantially modify the properties of the host crystal. In particular, charge transfer between the host and the intercalant modifies the occupation of the narrow conduction band of the host material (based on the Ta $5d_{z^2}$ level in TaS_2) and can radically change its electronic and optical properties [3]. The work to be described here concerns the 2H polytype of TaS_2 and its intercalates with magnetic 3d transition-metal ions—M_xTaS_2, where $x = \frac{1}{3}$ or $\frac{1}{4}$. At these concentrations of the intercalant, regular superlattices of 3d ions arise, with superlattice parameters parallel to the layers of $\sqrt{3}a$ and $2a$ respectively, where a is the host lattice parameter [4].

The band structure of the host material, calculated by Mattheiss [5] and more recently by Guo and Liang [6], is shown schematically in figure 1. It features a valence band based predominantly on the S 3p levels with a small contribution from the Ta 5d levels. Above

0953-8984/89/386865 + 11 $02.50

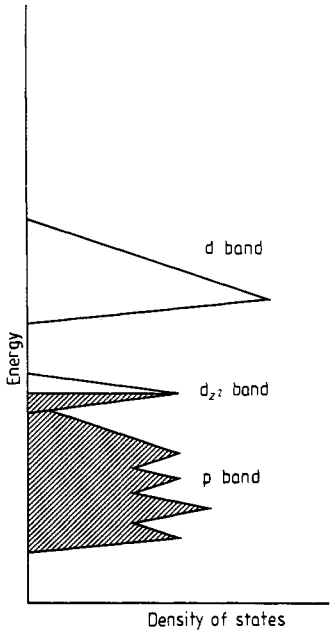

Figure 1. Schematic density of states of 2H-TaS_2.

this is the main Ta 5d band, which is split into two sections separated by a gap of about 1.4 eV. The lower of these is usually termed the d_{z^2} band, and has a capacity of two electrons per formula unit. The valence band is largely responsible for the strong intralayer bonding. The d_{z^2} band is half filled in the unintercalated host material, which is therefore metallic; the two-dimensional Fermi surface gives rise to charge density wave phenomena at low temperatures.

The electronic structures of the transition-metal intercalates are similar, but with one important modification; charge is transferred from the transition metal into the host conduction band, leaving the transition metal positively charged. For the Mn and Co intercalates discussed here, the intercalant atoms are known from paramagnetic susceptibility measurements [7] to be in a 2+ ionic state. The increase in ionicity strengthens the interlayer bonding and reduces the spacing between layers. The simplest picture of the charge transfer is the 'rigid band model' in which the band structure is assumed to be the same as that of the host material with the occupation of the d_{z^2} band increased by $2x$ electrons per formula unit. The lowering of carrier concentration caused by this shift of the Fermi energy can be seen in Hall coefficient data [4] and the model is further supported by XPS measurements of core level binding energies [8], and by photoemission studies of the valence bands of similar materials [9, 10].

The many-electron response associated with the screening of a core level hole produced in photoemission is well known to produce asymmetry in the core level lineshapes [11]; since the screening depends on the density of states close to the Fermi energy [12], the core level lineshapes in the materials studied here are likely to be affected by the increased occupation of the d_{z^2} band on intercalation. Because the density of states for the d_{z^2} band is so sharply peaked about its mid-energy (figure 1), the effects of band filling and the consequent marked reduction in the density of states at the Fermi energy should be pronounced. We report photoemission measurements on

the shallow Ta 4f core levels in the materials described above, and discuss the results in the light of model lineshape calculations based on the rigid band model.

2. Experimental procedure

Photoemission data was obtained for 2H-TaS_2 and two of its intercalates, $Mn_{1/4}TaS_2$ and $Co_{1/3}TaS_2$, using synchrotron radiation on beamline 6.1 at the SRS, Daresbury Laboratory, Warrington, UK. This employs a grazing incidence monochromator (GIM) for measurements in the 60–200 eV photon energy range. A cylindrical mirror analyser was used to obtain angle integrated spectra.

The crystals, typically 10 mm^2 in area, were fixed to a sample plate using a conducting epoxy and cleaved *in situ* with a chamber presure of 2×10^{-9} Torr or lower. The samples were grown by a vapour transport method usually employed for growth of transition-metal dichalcogenides [2]. Surface cleanliness was monitored using Auger electron spectroscopy and little contamination was observed. Low-energy electron diffraction patterns from the surfaces confirmed the presence of the intercalant superlattice for $Mn_{1/4}TaS_2$; no superlattice was visible for $Co_{1/3}TaS_2$, but subsequent x-ray diffraction analysis on the crystal confirmed the structure expected for this intercalant concentration.

Photoelectron spectra of the materials were obtained at room temperature using several photon energies. The structure of the spectra obtained did not change significantly with photon energy, so a photon energy of 80 eV was chosen for good overall energy resolution and acceptable count rate. A pass energy of 15 eV on the analyser gave a total resolution of 0.38 eV (monochromator and analyser combined, full width at half maximum).

3. Results and discussion

The energy distribution curves obtained for the Ta 4f core level for 2H-TaS_2, $Mn_{1/4}TaS_2$ and $Co_{1/3}TaS_2$ for a photon energy of 80 eV are shown in figure 2. The level is spin–orbit split by 1.88 eV, and the $4f_{7/2}$ and $4f_{5/2}$ component intensities are not in the expected 8 : 6 ratio, the $4f_{5/2}$ peak being 63% of the intensity of the $4f_{7/2}$. The asymmetric nature of the peaks is immediately obvious, each having a sharply defined high kinetic energy side, but with a tail extending a few eV to the low kinetic energy side. Even to the eye, it is clear that the asymmetry of the peaks decreases from 2H-TaS_2 through $Mn_{1/4}TaS_2$ to $Co_{1/3}TaS_2$. A shoulder on the low kinetic energy side of each peak in the 2H-TaS_2 and $Mn_{1/4}TaS_2$ spectra is also prominent, though this feature is absent in the case of $Co_{1/3}TaS_2$.

The asymmetry trend in the spectra requires a detailed explanation. In metals the conduction electrons tend to screen the core-level hole produced by the emission of the photoelectron, and this screening process gives rise to a range of many-electron excitations within the conduction band; the energy for these excitations is supplied by the kinetic energy of the photoelectron, so core-level lines often have a characteristic tail on the low kinetic energy side, and are consequently asymmetric. These peak asymmetries are well known experimentally, and are particularly marked for metals in which the density of states at the Fermi energy, which determines the total energy of such many electron excitations, is high. The core-level photoelectron lineshape of metals

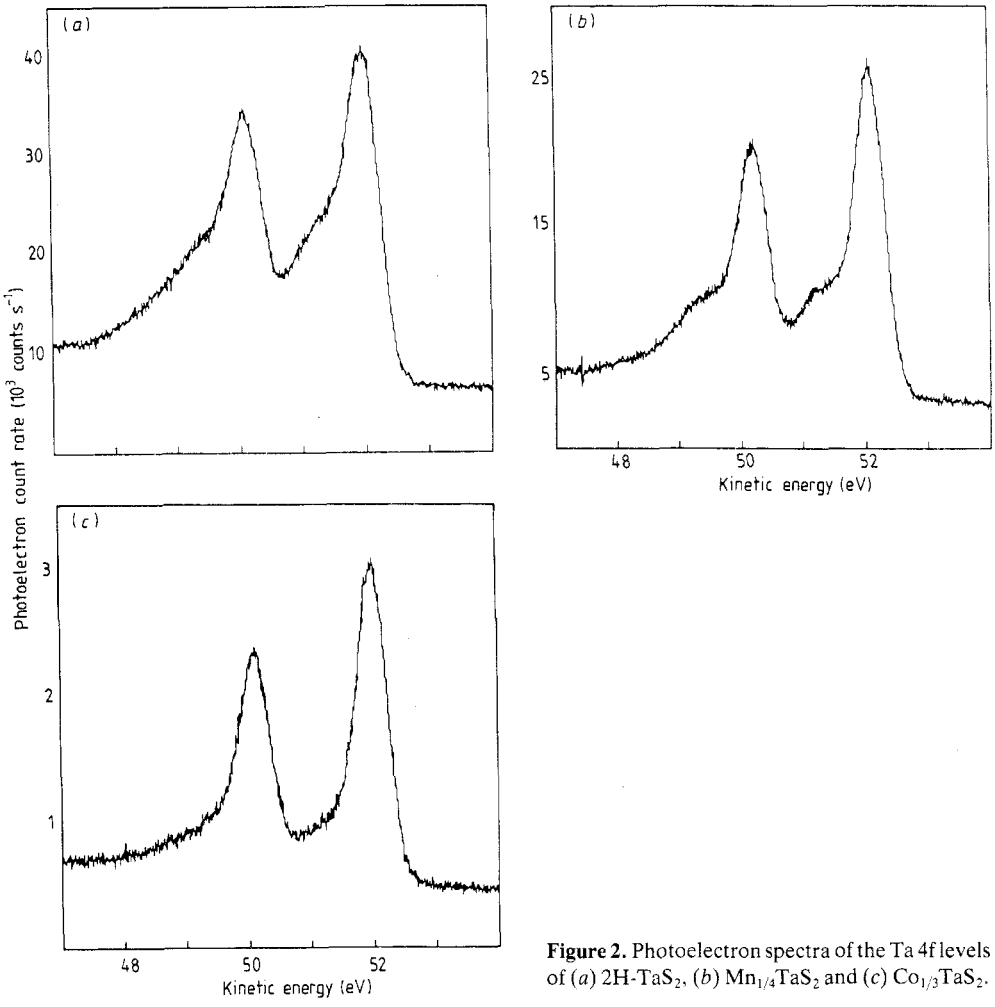

Figure 2. Photoelectron spectra of the Ta 4f levels of (*a*) 2H-TaS_2, (*b*) $Mn_{1/4}TaS_2$ and (*c*) $Co_{1/3}TaS_2$.

has been established by Nozières and De Dominicis [13] for the case in which the conduction electrons behave as s states of a free-electron gas. They solved the many-body problem exactly to show that the δ-function lineshape $E = \delta(E_0 - E)$ of a core-level line at kinetic energy $E = E_0$ is modified by the screening response of the conduction electrons to $E = (E_0 - E)^{\alpha - 1}$ for $E < E_0$, where α is an asymmetry parameter ($0 < \alpha < 1$) determined by the Friedel phase shifts. Doniach and Sunjic [14] have shown that a singularity of this form, when corrected for a line of non-zero lifetime width, appears in the photoelectron spectrum as an asymmetric lineshape (hereafter abbreviated as 'DS lineshape'). Though this lineshape is valid for low-energy excitations only, it has proved a good fit to experimental data up to a few eV from the line position E_0 [15]. The theory has been extended by Mahan [16] to energies further from E_0.

A more intuitive approach to the problem is taken by Hopfield [17], who obtains the result that $\alpha = V^2 N(E_F)^2$, where V represents an appropriate matrix element and $N(E_F)$ is the density of states at the Fermi energy. This leads to a simple explanation of the trend in asymmetries evident in figure 2. According to the rigid band model, the d_{z^2} band, the density of states of which peaks very close to the Fermi energy in 2H-TaS_2,

accommodates an extra $\frac{1}{2}$ electron per formula unit in $Mn_{1/4}TaS_2$ and an extra $\frac{2}{3}$ electron in $Co_{1/3}TaS_2$; the density of states at the Fermi energy will be correspondingly lowered because of the shape of the density states curve.

To quantify the change in asymmetry, the spectra have been subjected to a 'stripping procedure' to remove the contribution from the $4f_{5/2}$ and allow more extensive analysis of the $4f_{7/2}$ peak. This was done by subtracting a proportion of the $4f_{7/2}$ peak, offset by a spin–orbit splitting, from a spectrum. A single-pass subtraction was employed, using the result of the subtraction as it was evaluated and starting from high kinetic energy, defined by the transformation

$$C(E) \rightarrow C(E) - \gamma C(E + \delta)$$

where $C(E)$ is the count rate at energy E, γ is the proportion and δ the spin–orbit splitting. A deviation in either of the parameters γ or δ from its true value causes distortion in the form of oscillations at the lower kinetic energy end of the spectrum so these parameters were varied until the oscillations were eliminated. The error in γ is estimated to be 0.01 and in δ to be 0.02 eV or twice the energy spacing between sample points.

A 'least squares' routine was then used to find the best fit DS lineshape to the measured spectrum in the region very close to (i.e. within ~0.5 eV of) the peak. The 'stripped' data, and the fitted DS curves, appear in figure 3, and table 1 gives the final parameters used for the DS lineshapes. The parameters given in the table are not sensitive to the choice of γ and δ within reasonable limits. The DS lineshape with its inherent lifetime (Lorentzian) width has been broadened with a Gaussian of width 0.38 eV (full width at half maximum) as the instrumental resolution. As would be expected from direct inspection of the data, the asymmetry parameter (the parameter α in the DS lineshape) obtained by this procedure is markedly less in the intercalates than in the host compound.

In the case of $Co_{1/3}TaS_2$ the DS lineshape remains a good fit to the data several electron volts from the peak, while for the $Mn_{1/4}TaS_2$ spectrum the fit remains fairly good except in the region between 0.5 and 1.2 eV below the peak where the 'shoulder' occurs. However, the 2H-TaS_2 spectrum, besides showing a similar shoulder, drops clearly below the DS lineshape.

The shape of the tail on the low kinetic energy side of the peak requires further explanation, and it should be possible to relate the values of the asymmetry parameters to the electronic structure in terms of the rigid band model. The DS lineshape assumes that the conduction electrons are effectively free electrons and is readily applicable in cases such as alkali metals. But for a metal such as 2H-TaS_2 the conduction electrons are clearly not free. To treat such a system we use the approach taken by Hopfield [17] and developed by Wertheim and Citrin [18], though we make some simplifications. We consider the response of the conduction electrons as the response of independent electron–hole pairs to the perturbing potential of the core-level hole. For each possible electron–hole excitation of energy E_i the probability of excitation is given by

$$P_i = (V_i/E_i)^2 \tag{1}$$

where V_i is the matrix element of the perturbing core-hole potential for the excitation of energy E_i. So the probability distribution of losing energy E to this single excitation is

$$P(E) = [1 - (V_i/E_i)^2]\delta(E) + (V_i/E_i)^2\delta(E - E_i). \tag{2}$$

To find the spectrum of energy lost, we convolve the distributions like equation (2)

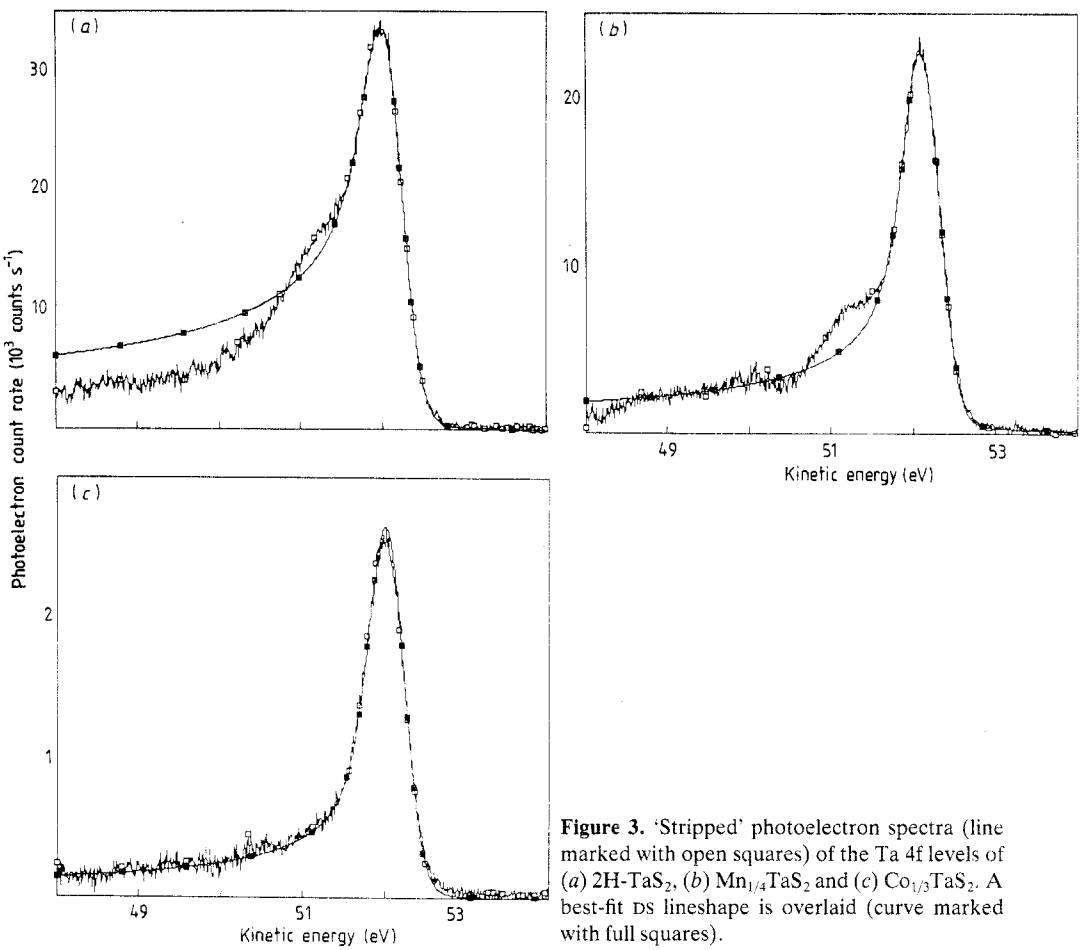

Figure 3. 'Stripped' photoelectron spectra (line marked with open squares) of the Ta 4f levels of (*a*) 2H-TaS_2, (*b*) $Mn_{1/4}TaS_2$ and (*c*) $Co_{1/3}TaS_2$. A best-fit DS lineshape is overlaid (curve marked with full squares).

Table 1. Lineshape parameters of the Ta 4f levels in 2H-TaS_2 and intercalates. Uncertainties in the last digit are shown in parentheses.

Compound	Kinetic energy (eV)	Binding energy (eV)	Lifetime width (eV)	Experimental asymmetry
2H-TaS_2	52.12(1)	22.73(5)	<0.04	0.46(1)
$Mn_{1/4}TaS_2$	52.17(1)	22.78(5)	<0.04	0.29(1)
$Co_{1/3}TaS_2$	52.08(1)	22.85(5)	<0.04	0.23(1)

for all possible excitations. Making a suitable approximation in the Fourier transform of $P(E)$ above and the simplistic assumption that the matrix elements for all excitations of energy E are equal, we obtain

$$P(E) = \int_{-\infty}^{\infty} \exp(\mathrm{i}Et) \exp\left(\int_0^{\infty} \frac{V^2(E')g(E')}{E'^2} (\exp(-\mathrm{i}E't) - 1)\, \mathrm{d}E' \right) \mathrm{d}t \tag{3}$$

where $g(E)$ is the density in energy of all the possible excitations, i.e. the joint density

of states for small excitations about the Fermi energy. It should be noted that equation (3) implicitly takes account of the possibility of multiple excitations. In fact, since the states involved in excitations differ in symmetry, the term $V^2(E')g(E')$ should be replaced by a decomposition into partial wave components

$$\sum_l V_l^2(E')g_l(E') \tag{4}$$

but we do not explicitly evaluate the matrix elements so this complication is ignored. Assuming that

$$g(E) \simeq N(E_F)^2 E \tag{5}$$

(which is the usual low-energy limit of g(E) and is exact for a free electron gas), we recover the result of Nozières and De Dominicis [13], a power-law electron–hole response

$$P(E) \simeq E^{\alpha-1} \qquad \text{with } \alpha = V^2 N(E_F)^2. \tag{6}$$

Wertheim and Walker [12] show that for a relationship of the form of equation (3), $P(E)$ depends only on the form of $V^2(E')g(E')$ in the region $E' < E$, implying that the power law will almost always be appropriate for low E.

We have evaluated equation (3) for the joint density of states expected for a half-filled d_{z^2} band as in 2H-TaS_2, with a model band structure of a triangular band, rather like that derived by Guo and Liang [6] in the vicinity of the Fermi energy, as shown in figure 4(a). The calculation was performed using fast Fourier transform algorithms using a 1024-point array. The expression was also evaluated for such a band filled, as predicted by the rigid band model, by the electrons transferred from the divalent intercalates with $x = \frac{1}{4}$ and $\frac{1}{3}$. Figure 4(b) shows the joint density of state functions associated with these model band structures. The matrix elements $V(E)$ have been taken as independent of energy E and the quantity $V(E)$ treated as an adjustable parameter. This parameter has been set so that with a density of states independent of energy and equal in value to the density of states at the top of the model band structure, the power-law lineshape $P(E) \simeq E^{\alpha-1}$ is obtained with an asymmetry parameter of 0.45, the same as the value obtained by fitting a DS lineshape to the experimental 2H-TaS_2 spectrum. This value for $V(E)$ has then been used with each of the joint density of states functions of figure 4(b).

In order to compare the results of this modelling directly with experiment it would be necessary to convolve numerically the lineshapes obtained from equation (3) with a Lorentzian to account for lifetime broadening and a Gaussian for instrumental broadening. However, the singularity at $E = E_0$ makes a numerical convolution unreliable. We have therefore chosen to display, in figure 5, the calculated lineshapes based on the model density of states shown in figure 4(a) alongside a power law of the form $E = (E_0 - E)^{\alpha-1}$ as expected for a density of states independent of energy. Neither takes account of any broadening. The asymmetry parameter α for these curves was chosen to give the closest apparent 'fit' to the calculated lineshape in the region E close to E_0. In each case, a curve with an asymmetry parameter differing from the one shown by 0.02 or more would have the wrong curvature to match the calculated lineshape in this region, hence we assign an uncertainty of 0.02 to the values of α arrived at in this way. Thus in figure 5 we have done for the lineshapes calculated from the model triangular density of states what in figure 3 we did for the experimental spectra themselves, that is, to compare them with lineshapes expected from a band structure consisting of a conduction band with a constant density of states and unlimited band width. The distinction is that in figure 3 there is broadening included, whereas in figure 5 there is none.

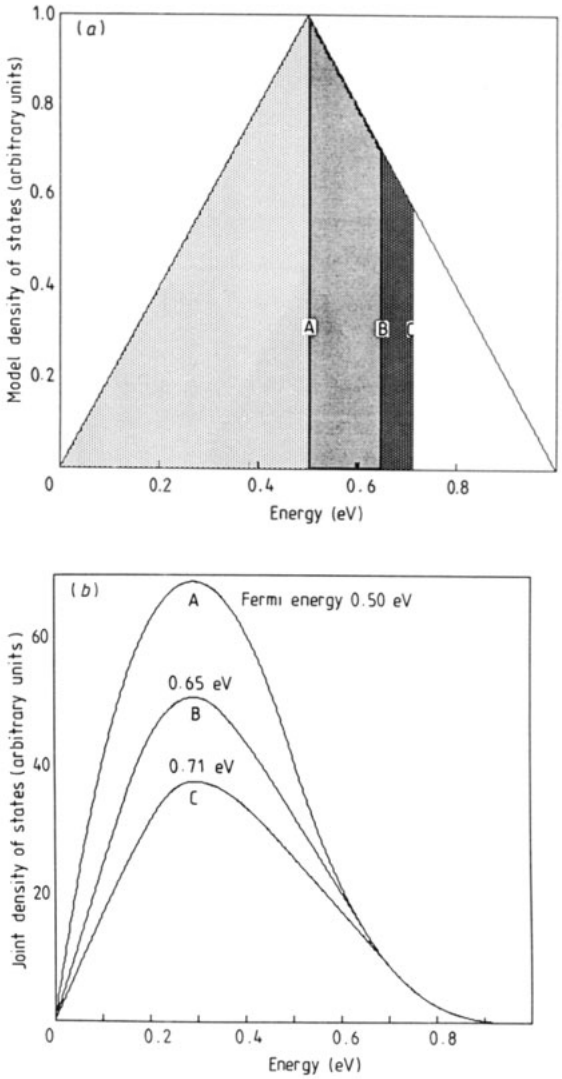

Figure 4. (*a*) Model density of states with Fermi energies marked as appropriate for 2H-TaS_2 (A), $Mn_{1/4}TaS_2$ (B) and $Co_{1/3}TaS_2$ (C) according to the rigid band model and (*b*) the corresponding joint densities of states calculated from these.

From figure 5 we can infer the following.

(i) In the vicinity of E_0 the $4f_{7/2}$ lineshape in the spectra of 2H-TaS_2 and its intercalates should be adequately fitted by a DS lineshape, since the lineshapes calculated from the model density of states of figure 4(*a*) are well fitted in this region by the power-law lineshapes. This is a consequence of the approximately linear behaviour of the joint density of states at low energy (<0.25 eV) for all the model density of states A, B, and C in figure 4(*b*). A material with a truly linear joint density of states would have exactly DS lineshape. This is clearly borne out in the data of figure 3. The DS lineshapes fit the experimental data very well in a region of 0.5 eV on either side of the peak.

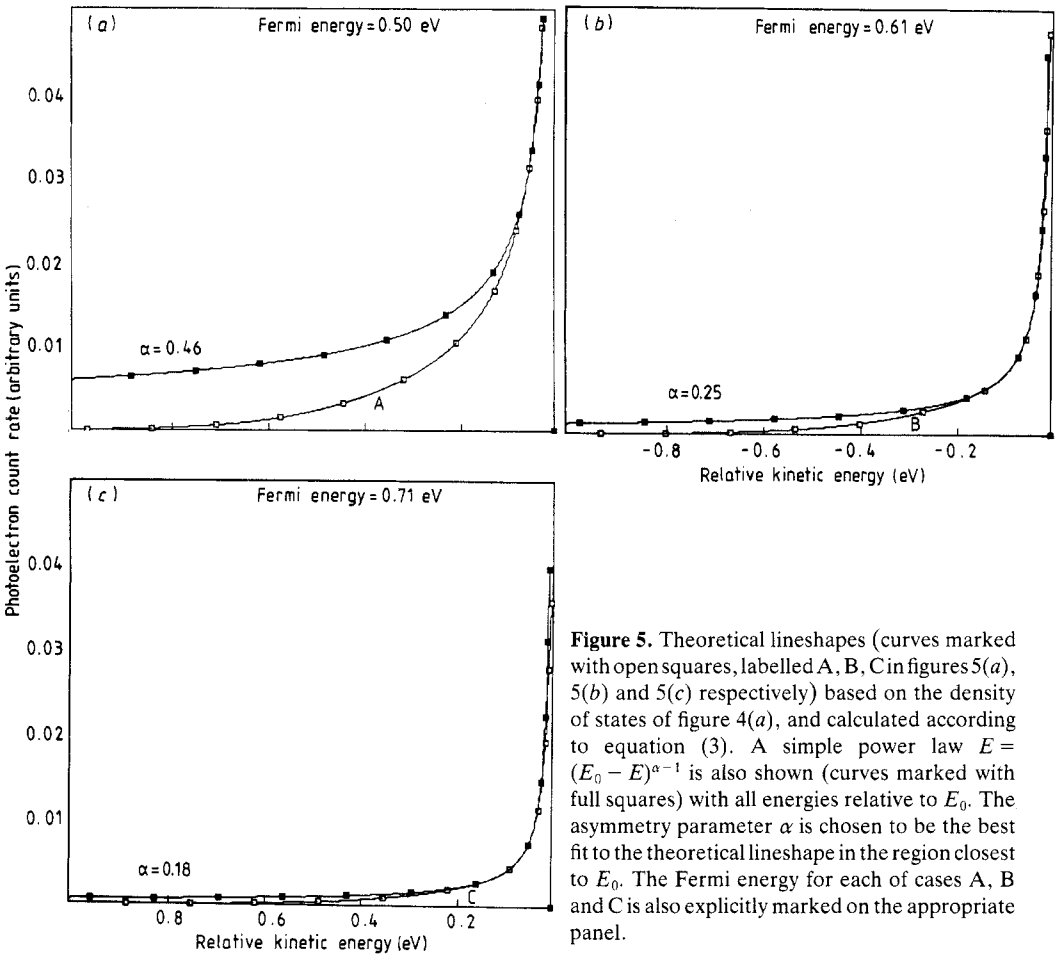

Figure 5. Theoretical lineshapes (curves marked with open squares, labelled A, B, C in figures 5(*a*), 5(*b*) and 5(*c*) respectively) based on the density of states of figure 4(*a*), and calculated according to equation (3). A simple power law $E = (E_0 - E)^{\alpha - 1}$ is also shown (curves marked with full squares) with all energies relative to E_0. The asymmetry parameter α is chosen to be the best fit to the theoretical lineshape in the region closest to E_0. The Fermi energy for each of cases A, B and C is also explicitly marked on the appropriate panel.

(ii) As the Fermi energy increases from the level in 2H-TaS_2 to the levels predicted by the rigid band model for $Mn_{1/4}TaS_2$ and for $Co_{1/3}TaS_2$, the asymmetry parameter of this DS lineshape should fall from 0.46 to approximately 0.25 and 0.18 respectively. This can be qualitatively understood as a lowering of the density of states $N(E_F)$ in equation (6). In the experimental data, as evident from table 1, the asymmetry parameters α fall to 0.29 in $Mn_{1/4}TaS_2$ and 0.23 in $Co_{1/3}TaS_2$. The correspondence is quite good, and the small discrepancy should be viewed as an inadequacy of the very simple triangular density of states used in figure 4(*a*) rather than as an imperfection of the rigid band model.

(iii) The close fit of the DS lineshape extends further in energy from the peak in the intercalates than in 2H-TaS_2. Whereas curve A in figure 5(*a*) representing 2H-TaS_2 falls below the power law lineshape only about 0.1 eV from the peak (or in this unbroadened case from the singularity at zero energy), curves B and C representing the intercalates are well approximated by the power law up to 0.2 to 0.3 eV from the peak. Again this is a consequence of the linearity of the joint density of states of figure 4(*b*). Curve A starts to drop below a straight line tangent at the origin before B or C do so. The experimental data confirms this, in that the 2H-TaS_2 lineshape of figure 3(*a*) falls below the DS

lineshape fairly close to the peak, whereas the intercalates lineshapes follow the DS for several electron volts. We discuss this further in (v) below.

(iv) There is no abrupt 'cut-off' in energy due to the width of the $5d_{z^2}$ band. Rather, the curves fall smoothly away from the power-law lineshape. It is therefore not possible to explain the shoulder at 0.9 eV below the peak in figures 3 in terms of a 'cut-off' in the electron–hole excitation spectrum imposed by the band structure, as might be presumed at first sight. The features are much too abrupt for this, and they are discussed further below.

(v) The tail should not extend more than 1 eV from the peak (about 1.25 eV from the peak when broadening is taken into account). This is not immediately obvious from the model band structures. Although no excitations of greater than 1 eV are possible, a mechanism involving multiple excitations could, at first sight, be responsible. However, the weight given in the lineshape to multiple excitations depends only on the size of the coupling constant $V(E)$ which is already determined by the shape of the line close to the peak. Even when multiple excitations are considered the line should fall to almost zero at energies more than 1 eV from the peak. The experiment tells a different story. In each case, the tail of the $4f_{7/2}$ peak extends several electron volts to the low kinetic energy side of the peak. The intercalates follow a DS lineshape, contrary to expectations, for much of this region. An obvious conclusion to draw from this is that the simple model of the density of states in the region of the Fermi level does not adequately represent the range of excitations available for the screening of a core level hole produced in photoemission.

Electron energy loss measurements [19] on 2H-TaS_2 and other transition-metal dichalcogenides show a plasmon excitation associated with the $5d_{z^2}$ band at about 1 eV. It therefore seems reasonable to attribute the satellite feature at 0.9 eV on the 2H-TaS_2 and $Mn_{1/4}TaS_2$ spectra with an extrinsic loss process, most likely the plasmon excitation observed in EELS. The complete absence of such a satellite in the $Co_{1/3}TaS_2$ spectrum remains unexplained, though the carrier concentration decreases as the band fills and its intensity would be expected to be less than in the other materials.

The joint density of states shown in figure 4(*b*) illustrate incidentally that the energy at which energy loss is greatest would not change much from 2H-TaS_2 to the intercalates, the peak in the curves A, B, and C is at the same energy. So the plasmon in $Mn_{1/4}TaS_2$ could well be of the same energy as that in 2H-TaS_2.

These extrinsic losses are unlikely to offer an explanation for the extended tails of the $4f_{7/2}$ peak. The lineshape in the extended region is plainly of the Doniach–Sunjic form and suggests a density of states much flatter than in figure 4(*a*) and much wider. The intercalant transition metal's remaining 3d electrons are believed to be localised and it is most improbable that they play a significant role in the screening of a core-level hole on the Ta. In intercalates involving tin and lead the 5p electrons of the intercalant radically change the nature of the density of states at the Fermi energy. In these materials the lineshapes might be expected to be much closer to DS lineshapes but an effect of this type in 3d transition metals is not likely.

An explanation involving the valence band electrons is more promising, though the region of low density of states between the 3p band and the $5d_{z^2}$ band (see figure 1) would give the line a very different character to the DS lineshape observed.

4. Conclusions

We have used angle-integrated photoemission to study the lineshapes of the Ta 4f levels of 2H-TaS_2, $Mn_{1/4}TaS_2$ and $Co_{1/3}TaS_2$. The lineshapes expected from a simple model of

the density of states have also been calculated. We find that the lineshapes are in accordance with those expected from a narrow band metal and that the asymmetries of the lineshapes are in general agreement with the rigid band model for the band structure of the intercalates. However, the extent of the tail caused by intrinsic losses cannot be adequately accounted for by electron–hole pair excitations within a simple model of the d_{z^2} band. There must be some other contribution to the density of states around the Fermi energy that participates in the screening of core level holes produced by photoemission. Some deviation from the simple model can be interpreted as an extrinsic loss of 0.9 eV, which is attributed to a bulk plasmon associated with the d_{z^2} band.

Acknowledgments

This work is supported by the UK Science and Engineering Research Council, and we are particularly grateful to the staff at the Daresbury SRS for their assistance with the photoemission measurements themselves.

References

[1] Beal A R 1979 *Intercalated Layered Materials* ed. F Lévy (Dordrecht: Reidel)
[2] Wilson J A and Yoffe A D 1987 *Adv. Phys.* **18** 193
[3] Friend R H and Yoffe A D 1987 *Adv. Phys.* **36** 1
[4] Parkin S S P and Friend R H 1980 *Phil. Mag.* B **41** 65
[5] Mattheiss L F 1973 *Phys. Rev.* B **8** 3719
[6] Guo G Y and Liang W Y 1987 *J. Phys. C: Solid State Phys.* **20** 4315
[7] Parkin S S P and Friend R H 1980 *Phil. Mag.* B **41** 65
[8] Barry J J and Hughes H P 1982 *J. Phys. C: Solid State Phys.* **15** L797
[9] Clark W B 1976 *J. Phys. C: Solid State Phys.* **9** L693
[10] Barry J J and Hughes H P 1983 *J. Phys. C: Solid State Phys.* **16** 5393
[11] Wertheim G K and Hüfner S 1975 *Phys. Rev. Lett.* **35** 53
[12] Wertheim G K and Walker L R 1976 *J. Phys. F: Met. Phys.* **6** 2297
[13] Nozières P and De Dominicis C T 1969 *Phys. Rev.* **178** 1097
[14] Doniach S and Sunjic M 1970 *J. Phys. C: Solid State Phys.* **3** 285
[15] Citrin P H, Wertheim G K and Baer Y 1975 *Phys. Rev. Lett.* **35** 885
[16] Mahan G D 1975 *Phys Rev.* B **11** 4814
[17] Hopfield J J 1969 *Comment. Solid State Phys.* **2** 40
[18] Wertheim G K and Citrin P H 1978 *Photoemission in Solids* vol 1, ed. M Cardona and L Ley (Berlin: Springer)
[19] Beal A R, Hughes H P and Liang W Y 1975 *J. Phys. C: Solid State Phys.* **8** 4236